24-035

Enrichment Feasibility of Tellurium, Gold, and Silver from Copper Tailings

Jose L. Corchado-Albelo
Missouri University of Science & Technology,
Rolla, MO, USA

Lana Alagha
Missouri University of Science & Technology,
Rolla, MO, USA

Fardis Nakhaei
Missouri University of Science & Technology,
Rolla, MO, USA

ABSTRACT

Tellurium (Te), a critical mineral for solar energy technologies, faces supply risk challenges that drive the development of diversified and robust production routes. This research focused on improving Te enrichment from copper tailings (CT) produced from copper porphyry (CP) ores processing, addressing the loss of ~90% of Te minerals to tailings in the flotation process of CP ores. Gravity separation and froth flotation processes were used as possible enrichment routes of Te-bearing minerals (i.e., pyrite) in CT. In the froth flotation process, synergistic combinations of reagents were tested to achieve an acceptable enrichment ratio of Te minerals. Comprehensive characterization analyses showed significant Te enrichment in the flotation concentrates. Tellurium was recovered at 90%, while the grade of Te in the concentrates was 1.4 ppm using a xanthate collector and glycol frother compared to <0.5 ppm in the flotation feed. Findings showed that Te-minerals' enrichment was also feasible in CT using the proposed combined concentrations routes (i.e., gravity separation followed by froth flotation) by looking at Fe, Cu, and S enrichment. This study also highlighted the importance of understanding the deportment of Te minerals in different process streams to develop and optimize efficient enrichment practices.

INTRODUCTION

Tellurium (Te) is a critical mineral in many governmental strategic mineral lists, such as the U.S.A., Canada, United Kingdom, Japan, and India [1–6]. Critical minerals are specific commodities categorized by a government or the private sector because of instability and risks to the supply chain due to trade exposure, supply disruption potential, and economic vulnerability [7–13]. Since the early 2010s, critical minerals have resurged as an issue of interest for research and development because of unstable supply chains, trade exposure, and economic vulnerability of specialized commodities [7,11,13]. The change in the commodity supply chains associated with the transition from fossil fuels to more sustainable energy sources is of increased concern when looking at secure and ethical sourcing/supply of specialized commodities. Consequently, many world governments and private sectors name these elements or commodities as critical minerals [11,14–20]. Tellurium has gained increasing attention in the last decade due to its importance to clean solar energy production, most notably as an essential raw material in cadmium telluride (CdTe) photovoltaic applications. In recent years, the demand for Te has increased as it continues to be incorporated into manifold specialized applications. For example, Te is an additive to metal alloys in glass optical fibers, ceramics as a

pigment and catalyst, magnetic discs, and solar panel applications [21,22].

Furthermore, Te is only economically recoverable from copper porphyry deposits using complex production processes [14,23–25]. Statistical data from 2000 to 2020 shows that 90% of Te production occurs as a by-product of copper porphyry deposit anode slimes reprocessed by refining [22,23].

Literature suggests other production routes for Te, such as the copper porphyry flotation streams, where 60 – 90% of tellurium in the system is deported to the tailings or non-copper-producing streams [9]. A study of the flotation streams of a large copper porphyry concentrator in the U.S.A. suggested that 88% of Te available in the flotation streams was deported to the tailings. This study also indicated that Te deported to the tailings was locked in larger pyrite grains and associated with Au-Ag minerals [26].

Therefore, this study investigated the potential of different enrichment practices to recover Te minerals lost/deported to copper tailings from operating copper mines. Additionally, the study examined the mineralogy and deportment of telluride minerals in CT and post-processing streams for enrichment and enhanced recovery of Te. The methodologies used for the characterization of CT for tellurides and composition were inductively coupled plasma-mass spectrometry (ICP-MS), X-ray fluorescence (XRF), and TESCAN's Integrated Mineral Analysis (TIMA). The strategies proposed for the enrichment and enhanced recovery of tellurides were baseline pyrite/sulfide flotation experiments using carbamate (EXP300422) and xanthate (SIPX) collectors, and glycol (OREPREP X-237), methyl isobutyl carbinol (MIBC) and terpineol frothers. Lastly, gravity separation and froth flotation experiments were used as a combined approach that would produce a higher-grade pyrite/sulfide concentrate.

MATERIALS

Tailing Samples and Reagents

The copper tailings (CT) samples consisted of rougher tailings grab samples from a large copper producer in the U.S.A. The samples were air-dried and further split into representative portions for flotation and gravity separation experiments.

Flotation Reagents

Reagents such as carbamate (EXP300422) and xanthate (SIPX) collectors, and glycol (OREPREP X-237) frother were obtained from Cytec Industries (Solvay), and stock solutions were prepared at 1g/L. Frothers such as methyl isobutyl carbinol (MIBC) and terpinoel were purchased from Fisher Scientific, and a stock solution was prepared at 1 g/L. Sodium hydroxide (NaOH) and hydrochloric acid (HCl) were purchased from Fisher Scientific and used for pH modification from prepared stock solutions of 10 g/L and 9.12 g/L solutions, respectively.

RESEARCH METHODS

Characterization of Copper Tailings

TESCAN'S Integrated Mineral Analysis Studies

TESCAN's Integrated Mineral Analysis (TIMA) was performed on CT to identify the mineral associations and locking behavior for different REEbearing mineral phases. TIMA was conducted at Montana Technological University's Center for Advanced Materials Processing (CAMP) using a polished epoxy mount of the copper tailings sample. The sample was prepared for automated phase analysis by scanning electron microscopy-energy dispersive Xray (SEM-EDS) using TIMA software [27].

Characterization of Flotation and Gravity Separation Experiments

X-Ray Fluorescence Studies

The samples were prepared -38 µm by abrasion. Tests were performed in an energy dispersive x-ray fluorescence (XRF) device with a 5sample carrousel. XRF characterization identified and quantified the elemental content based on the resulting X-ray fluorescence. The XRF was performed to identify iron, copper, and sulfur in the CT, flotation concentrates, flotation tailings, gravity separation (GS) tailings, GS concentrates, and GS middling samples [28].

Inductively Coupled Plasma—Mass Spectrometry Studies

The inductively coupled plasma mass spectrometry (ICP-MS) was performed to identify tellurium and other valuables in the CT (experimental feed), flotation concentrates, and flotation tailings samples. ICP-MS "total" digestion process was used to test digested powdered mineral samples in a fourstep dilution process beginning with hydrochloric acid, second nitric acid, third perchloric acid, and lastly, hydrofluoric acid. The digestion produced a stable ionic solution used for ICP-MS analysis [29].

BASELINE FLOTATION EXPERIMENTS

Bulk sulfide flotation experiments were conducted to establish a baseline and feasibility of concentrating tellurium-bearing minerals from the CT samples. The selected sulfide collectors were EXP300422 and SIPX. Flotation experiments were carried out in a Denver D12 flotation machine

Table 1. Baseline Flotation Experiment Design

Description	Collector Dosage (g/ton)
EXP300422 + MIBC	30, 60, 90, 120, 150 & 180
EXP300422 + OREPREP X-237	90 & 150
EXP 300422 + terpineol	90 & 150
SPIX + MIBC	30, 60, 90, 120, 150 & 180
SPIX + OREPREP X-237	90 & 150
SPIX + terpineol	90 & 150

with the 1L cell and the 2-7/8 in. diameter impeller attachment. These experiments were performed using procedures published in the literature for similar systems[30,31]. The flotation feed (P_{80} = 135µm, P_{50} =42 µm) was prepared in tap water at 30 wt.% solids. The prepared slurry was agitated at 900 RPM for 3 mins. The slurry's pH was modified to pH 9 using NaOH. The frother's dosage was fixed at 50 g/t for all experiments. Table 1 shows the parameters and conditions used in this set of feasibility experiments. The experiments were performed with pH conditioning, followed by collector addition, and lastly, the frother at the specified dosages.

Concentrates were collected over 5 min. of flotation time. The concentrate and tailing products were dried, weighed, and assayed using ICP-MS. Recovery was calculated using Equation 1.

$$R(\%\ \text{element or compound}) = \frac{Cc}{(C * c + Tt)} * 100 \qquad (1)$$

In Equation 1, C is the mass of the concentrates, c is the grade of valuable element or compound in the concentrates, T is the mass of the tailings, and t is the grade of valuable element or compound in the tailings. Flotation enrichment was calculated using concentrate grade over feed grade.

Preconcentration and Flotation Experiments

Based on the results from the baseline experiments, preconcentration experiments were conducted using a Wilfley Table by Outotec (Equation 1). Preconcentration experiments used the Wilfley Table for gravity separation (GS) and production of three streams: concentrate, middlings, and tailings. The preconcentration experiments aimed to deslime the CT (as-received material). The process consisted of performing 3 GS experiments by increasing the solid-liquid ratio from 1:15, 1:10, and 1:5. The remaining GS parameters were consistent at 11 cm stroke, 0° tilt (flat), slurry flow of 1.2 L/min. and wash water flow 1 L/min. The middlings and the concentrate streams were combined to generate a preconcentration product used in the flotation experiments using the most efficient collector and frother combination from the baseline experiments. Figure 1 shows the proposed telluride concentration strategies.

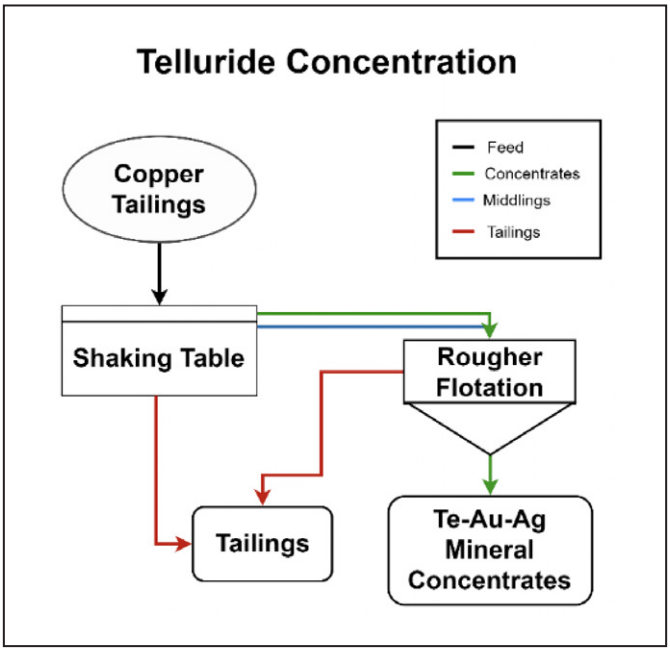

Figure 1. Copper tailings preconcentration strategies followed by flotation of concentrate and middling mix to produce an Au-Ag-Te rich concentrate

All the grades for these streams were quantified using XRF. The recoveries for the flotation and preconcentration experiments were calculated using Equation 1. Flotation enrichment was calculated using concentrate grade over feed grade.

RESULTS

Characterization of Copper Tailings

Chemical Composition of Copper Tailings

The average concentration of tellurium, gold, and silver in CT was determined using ICP-MS. Tellurium, gold, and silver grades were 0.4 ppm, 61.7 ppb, and 0.66 ppm, respectively. The name "valuable elements" was given to commodities that would positively impact the process if these elements were concentrated with Te by flotation. Furthermore, other elements were placed in the valuable elements list because they are part of the U.S.A. critical mineral list. The remaining grades for valuables considered are shown in Table 2.

Additionally, XRF analysis was performed on CT samples and averaged to obtain a general distribution of major elements that contribute to the composition of CT. Major elements have >1 wt.%, minor elements have a 0.1 wt.% to 1 wt.%, and trace elements have <0.1 wt.% composition.

Table 2. ICP-MS of valuable elements in CT samples, where the values are the average of 3 as received CT batches.

Valuable Elements	Assays
Te	0.40 ppm
Au	61.70 ppb
Ag	0.66 ppm
Cu	494.50 ppm
Mo	40.43 ppm
Pb	33.32 ppm
Ni	39.18 ppm
Zn	40.77 ppm
S	1.50 %
As	12.85 ppm
Bi	1.08 ppm
Co	17.03 ppm
Fe	4.12 %
Ga	18.23 ppm
Ge	0.10 ppm
Se	2.13 ppm

The major elements composing CT were Si, Fe, Al, Sb, Ti Sn, and S with a grade of 47.34 wt.%, 22.12 wt.%, 17.80 wt.%, 5.60 wt.%, 2.72 wt.%, 1.98 wt.%, and 1.11 wt.%. The XRF composition of the CT samples is shown in Table 3.

Automated Mineralogy of Copper Tailings

TESCAN's Integrated Mineral Analysis (TIMA) showed a particle size distribution analysis (PSD) of P_{80} of 135 µm and a median size of 42 µm CT samples. TIMA was used to identify the major mineral classes as 91.1% silicates (16.8% are phyllosilicates), 3.91% sulfides (0.09% are Cusulfides), 2.25% carbonates, 1.83% oxides and hydroxides, and 0.83% phosphates. Furthermore, the modal distribution of the major minerals in CT were gangue minerals with 36.5% quartz, 23.6% K-

Feldspar, 14.2% biotite, 5.13% albite, 2.23% calcite, 2.17% plagioclase, 2.0% Ca-Mg pyroxenes, 2.03% anorthoclase, 1.86% andradite, 1.55% muscovite and 1.53% hematite/magnetite. Pyrite was the primary sulfide at 3.82%, followed by chalcopyrite at 0.08% in CT.

However, the scan of the as-received samples did not detect any of the Te, Au, and Ag minerals; therefore, a gravity concentration step was performed using a Mozley Laboratory Mineral Separator using approximately 50 grams of material with particles less than 100 µm to concentrate Te-Au-Ag phases. The concentrates from the gravity-separated CT were analyzed using TIMA bright phase analysis, and minerals of interest were identified as native gold, electrum, petzite, hessite/argentite, goldfieldite, and tetradymite. The major mineralogical composition of the

Table 3. XRF elemental composition of CT samples, where the values are the average of 3 as received CT batches.

Element	Grade (wt. %)
Al	17.80
Si	47.34
P	0.32
S	1.11
Ti	2.72
V	0.12
Mn	0.15
Fe	22.12
Co	0.04
Ni	0.03
Cu	0.29
As	0.01
Zr	0.33
Mo	0.02
Sn	1.98
Sb	5.60
Pb	0.03

Table 4. Bright-phase analysis of the Mozley concentrates using TIMA. ND = not detected.

Mineral	Formula	Mozley Conc. CT (wt.%)
Pyrite	FeS_2	84.75
Galena	PbS	1.67
Chalcopyrite	$CuFeS_2$	0.14
Hematite / Magnetite	Fe_2O_3/Fe_3O_4	2.055
Tennantite	$(Cu,Fe,Zn)_{12}As_4S_{13}$	0.27
Tetradymite	Bi_2Te_2S	0.065
Hodrushite	Cu4Bi6S11	0.01
Petzite	Ag_3AuTe_2	0.03
Hessite	Ag_2Te	0.02
Goldfieldite	$Cu_{12}(Sb,Te)_4S_{13}$	0.01
Gold	Au	0.009
CuNi Sulfides	$Cu_xNi_yS_z$	0.01
Tetrahedrite	$(Cu,Fe,Zn)_{12}(Sb,As)_4S_{13}$	0.009
Electrum	$Au_{0.8}Ag_{0.2}$	ND
Laitakarite	$Bi_4(Se,S)_3$	ND

CT Mozley concentrates was 84.75% pyrite, 2.06% hematite/magnetite, and 1.67% galena. Table 4 presents the mineralogical distribution of the Mozley concentrates of CT using TIMA bright-phase analysis, excluding silicates, phosphates, and carbonates.

As determined by TIMA, elemental distribution for Te by mineral phase in CT showed that tetradymite contained the largest Te abundance of 75.3% Te. Tellurium was distributed into the other mineral phases: 15% petzite, 9.2% hessite, and 0.5% hessite. Gold elemental distribution, as

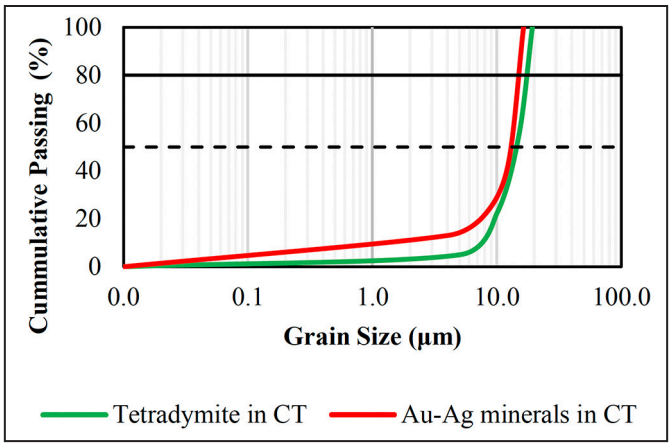

Figure 2. Particle size distribution of tetradymite and Au-Ag minerals showing P_{80} with a straight black line and P_{50} or median as a dashed black line.

determined by TIMA, showed that the largest Au abundance of 69.8% corresponded to native gold, followed by 30.2% Au abundance in petzite.

Mineral liberation analysis of CT using TIMA indicated that Te minerals (using tetradymite as a Te representative) and Au-Ag minerals were very fine-grained sized, with 100% of the grains less than 20 µm. The PSD of tetradymite and Au-Ag grains showed that P_{80} was 14 µm and 16 µm, respectively. The PSD for tetradymite and Au-Ag minerals as a function of increasing size (log_{10}-scale) and cumulative passing in Figure 2.

Furthermore, liberation analysis of CT using TIMA indicated that tetradymite and Au-Ag minerals were primarily locked in pyrite, as less than 20 µm inclusions. Tables 5 and Figure 3 show that pyrite hosted both tetradymite and Au-Ag minerals at least 93%, with at least 3% of both reporting as free surface minerals.

TIMA of CT suggested that Te, Au, and Ag minerals were primarily hosted in pyrite as less than 20 µm inclusions. Therefore, this research investigated whether reprocessing of CT using a bulk pyrite flotation process could be a feasible strategy to increase Te recovery from the existing copper porphyry supply chain [26,31,32].

Table 5. Liberation analysis of Te, Ag, and Au minerals in CT

Mineral	Tetradymite Locking (wt.%)	Au-Ag mineral Locking (wt.%)
Pyrite	94.7	93.3
Apatite	0.1	0
Hematite/agnetite	1.5	0.9
Calcite	0.2	0
Free surface	3.3	5.7

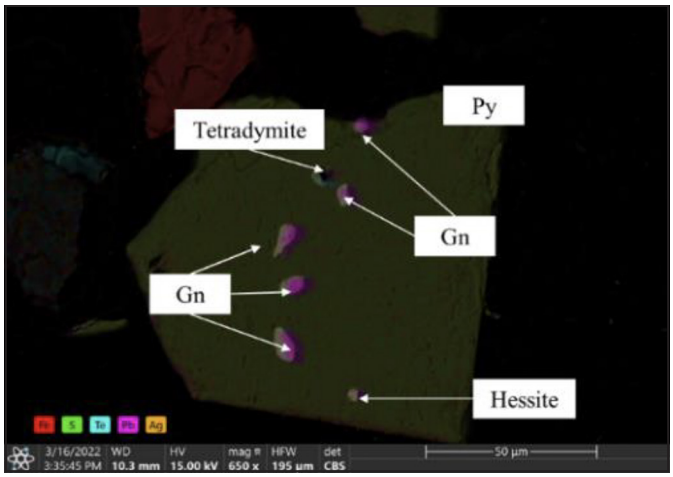

Figure 3. False-color SEM-EDS of a 120 µm pyrite (Py) grain in CT Mozley concentrates. The pyrite grain locked at least 7 inclusions less than 30 µm, of which 5 were galena (Gn), and the remaining were tetradymite and hessite/argentite

Bench-Scale Flotation Experiments

The flotation efficiency of Te, Au, and Ag minerals (presented as Te, Au, and Ag concentrations in concentrate products) was investigated using EXP300422 and SIPX collectors and OREPREP X237, MIBC, and terpineol frothers. The results from the baseline experiments showed that the most efficient reagent combination for recovering Te was 150 g/t SIPX with 50 g/t OREPREP X-237, achieving a 92.18% recovery at 1.4 ppm. The most efficient reagent combination for recovering Au was 30 g/t SIPX with 50 g/t MIBC, achieving a 79.37% recovery at 121 ppb. Lastly, the most efficient reagent combination for recovering Ag was 150 g/t SIPX with 50 g/t terpineol, achieving a 91.15 % recovery at 0.99 ppm.

Notably, from the reagent combinations mentioned before, the reagent combination that achieved the highest overall efficiency was 150 g/t SIPX with 50 g/t OREPREP X-237. For this reagent combination, Te, Au, and Ag recovery were 92.18%, 74.55 and 76.97%, respectively. Tellurium, Au, and Ag grades were also 1.4 ppm, 160 ppb, and 1.23 ppm, respectively. Figure 4 summarizes the baseline test results, highlighting the most efficient collector and frother combinations for Te, Au, and Ag.

Results showed in Table 6 that the collector and frother combinations positively impacted the flotation recovery of Te in the following order: SIPX > EXP300422 and OREPREP > terpineol > MIBC. Collector and frother combination positively impacted Au recovery in the following order: SIPX > EXP 300422 and MIBC > OREPREP X-237 > terpineol. Lastly, Ag recovery was positively affected by the collector frother combination in the following order:

Table 6. Results from Baseline Flotation Experiment Testing Synergistic Collector and Frother Combinations

Description of Collector and Frother Dosage	Au Grade (ppb)	Au Recovery (%)	Ag Grade (ppm)	Ag Recovery (ppm)	Te Grade (%)	Te Recovery (ppm)
EXP300422 (30 g/t) + MIBC (50 g/t)	76	49.6	0.8	53.8	0.6	51.8
EXP300422 (60 g/t) + MIBC (5 0g/t)	60	53.7	0.8	58.9	0.7	67.7
EXP300422 (90 g/t) + MIBC (50 g/t)	71	61.2	0.8	62.0	0.6	59.8
EXP300422 (120 g/t) + MIBC (50 g/t)	97	66.5	0.9	61.0	0.9	63.4
EXP300422 (150 g/t) + MIBC (50 g/t)	87	67.2	0.8	62.9	0.8	71.0
EXP300422 (180 g/t) + MIBC (50 g/t)	62	57.5	0.8	57.6	1.1	71.6
EXP300422 (90 g/t) + terpineol (50 g/t)	135	64.2	1.3	66.3	1.2	86.1
EXP300422 (150 g/t) + terpineol (50 g/t)	79	66.6	1.1	67.1	1.2	90.9
EXP300422 (90 g/t) + OREPREP X-237 (50 g/t)	125	64.5	1.1	68.1	1.4	80.3
EXP300422 (150 g/t) + OREPREP X-237 (50 g/t)	152	77.5	1.1	66.2	1.3	79.3
SPIX (30 g/t) + MIBC (50g/t)	121	79.4	0.8	60.9	0.8	67.0
SIPX (60 g/t) + MIBC (50g/t)	85	42.7	0.8	43.9	0.9	54.6
SIPX (90 g/t) + MIBC (50g/t)	64	53.9	0.8	67.1	0.7	73.3
SIPX (120 g/t) + MIBC (50g/t)	86	60.2	0.8	59.4	0.8	67.5
SIPX (150 g/t) + MIBC (50g/t)	49	63.2	0.9	63.3	0.8	72.2
SIPX (180 g/t) + MIBC (50g/t)	75	53.8	0.8	60.6	0.7	66.8
SIPX (90 g/t) + OREPREP X-237 (50 g/t)	117	67.0	1.4	78.8	1.3	91.7
SIPX (150 g/t) + OREPREP X-237 (50 g/t)	160	74.6	1.2	92.0	1.4	92.2
SIPX (90 g/t) + terpineol (50 g/t)	92	68.6	1.2	75.6	1.3	91.3

SIPX > EXP 300422 and OREPREP X-237 > terpineol > MIBC.

Therefore, the relationships between the collector dosage and frother combination provided a successful recovery of >90% tellurium; however, these high recoveries were achieved at very low grade (<1.4 ppm) and a high mass pull incorporating a large volume of gangue minerals.

This research proposed using a combination of GS and flotation using xanthate collectors and glycol frother to obtain a cleaner pyrite-sulfide concentrate, which will concentrate Te, Au, Ag, and other values from CT.

PRECONCENTRATION AND FLOTATION EXPERIMENTS FOR COPPER TAILINGS

Preconcentration Using Gravity Separation

The preconcentration experiments first tested the recovery of Fe, Cu, and S by examining the GS solid-liquid ratio parameter.

Results from the GS experiment 1 with a 1:15 solid-liquid ratio (GS 1) showed that the highest recoveries were achieved in the middlings, with similar distribution in the concentrate and tailings. Iron recovery was 24.50%, 39.43%, and 30.69% in the concentrates, middlings, and tailings, respectively. Copper recovery was 30.56%, 40.45%, and 22.98% in the concentrates, middlings, and tailings, respectively. Sulfur recovery was 31.22%, 34.56%, and 27.30% in the concentrates, middlings, and tailings, respectively. The combined middlings and concentrate mass recovery was 65.22 wt.%.

GS experiment 2 with a 1:10 solid-liquid ratio (GS 2) showed that the highest recoveries were achieved in the concentrates. Iron recovery was 29.01%, 35.58%, and 31.86% in the concentrates, middlings, and tailings, respectively. Copper recovery was 35.37%, 30.34%, and 30.45% in the concentrates, middlings, and tailings, respectively. Sulfur recovery was 35.75%, 30.67%, and 30.78% in the concentrates, middlings, and tailings, respectively. The combined middlings and concentrate mass recovery was 66.44 wt.%.

GS experiment 3 with a 1:5 solid-liquid ratio (GS 3) showed that the highest recoveries were achieved in the tailings, with similar distribution in the concentrate and middlings. Iron recovery was 9.88%, 11.38, and 70.36% in the concentrates, middlings, and tailings, respectively. Copper recovery was 18.35%, 11.71%, and 60.67% in the concentrates, middlings, and tailings, respectively. Sulfur recovery was 16.47%, 12.76%, and 60.08% in the concentrates, middlings, and tailings, respectively. The combined middlings and concentrate mass recovery was 51.08 wt.%.

The results from the GS experiments informed the decision to use the GS concentrate and middling (GS-C+M)

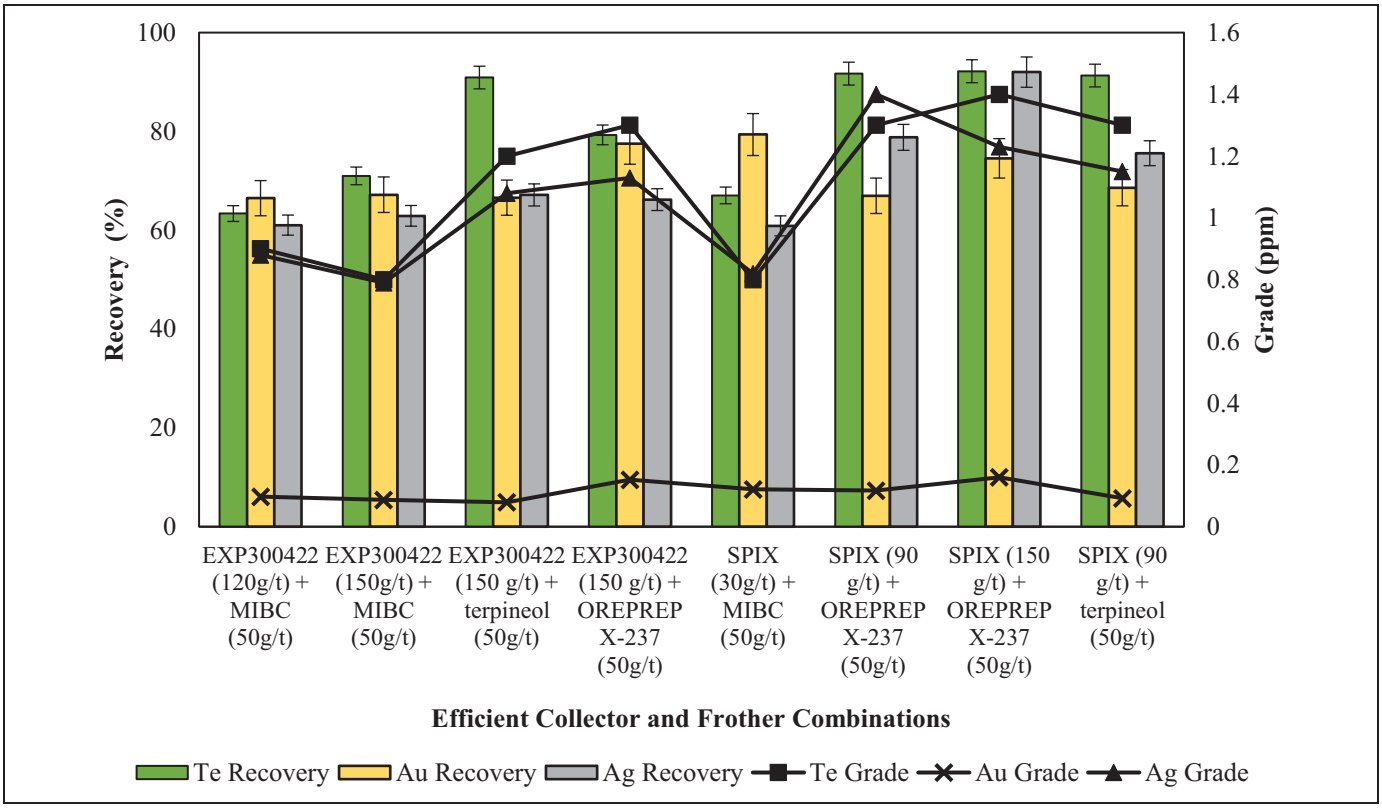

Figure 4. Efficiency of collector type, dosage, and frother type combinations as a function of recovery and grade. Recovery (%) is represented by green (Te), light gold (Au), and light gray (Ag) columns, while the grade for Te is a square, Au is an X, and Ag is a triangle

combined as the flotation feed after preconcentration. The high mass recovery in the GS-C+M and the desliming (that produced higher pyrite flotatbility) suggested an enhanced recovery of Te, Au, and Ag because of the positive locking relationship that tellurides exhibited in pyrite.

Flotation of Preconcentrated Copper Tailings

Pyrite bulk flotation was performed at the bench-scale level using the GS-C+M, and the recovery and grade from these experiments are shown in Figures 5–7. For this set of experiments and based on the results obtained from the baseline flotation, the researchers opted to float GS-C+M as a function of the lowest dosages tested for xanthate (SIPX) collector and glycol (OREPREP X-237) frothers. The dosage selected for the collector was 90 g/t, and the frother was 50 g/t.

Results showed that flotation of GS 1-C+M had the highest overall recovery of Fe and S. Sulfur recovery was 52.99% at a grade of 1.84 wt.%. Iron recovery was 29.60% at a grade of 24.24 wt.%. GS 3- C+M had the highest overall recovery of Cu, with 59.83% recovery at 4.68 wt.%. The results highlighted a cleaner concentrate product with higher Cu and S grades.

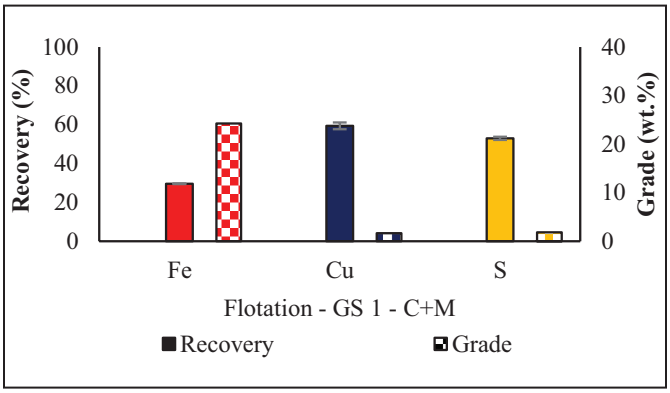

Figure 5. Flotation recovery and grade of the concentrate and middlings of gravity separation with a 1:15 S/L ratio

DISCUSSION

The research findings presented a comprehensive picture of the recovery, grades, and enrichment percentages of tellurium (Te), gold (Au), silver (Ag), and copper (Cu) from copper tailings (CT). Initially, the characterization of the tailings provided a baseline understanding of the starting grades, with Te at 0.40 ppm, Au at 61.7 ppb, Ag at 0.66 ppm, and Cu at 494.50 ppm. This research and

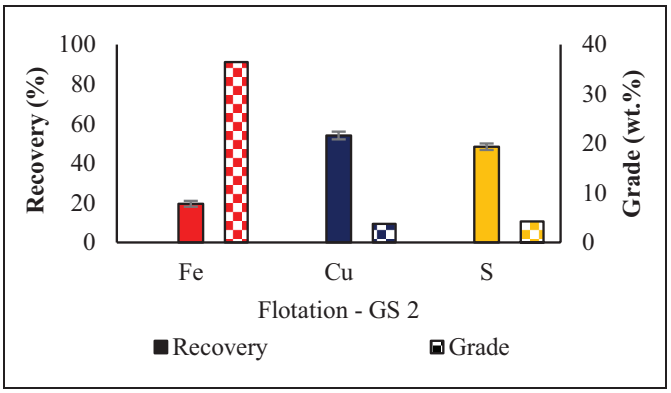

Figure 6. Flotation recovery and grade of the concentrate and middlings of gravity separation with a 1:10 S/L ratio.

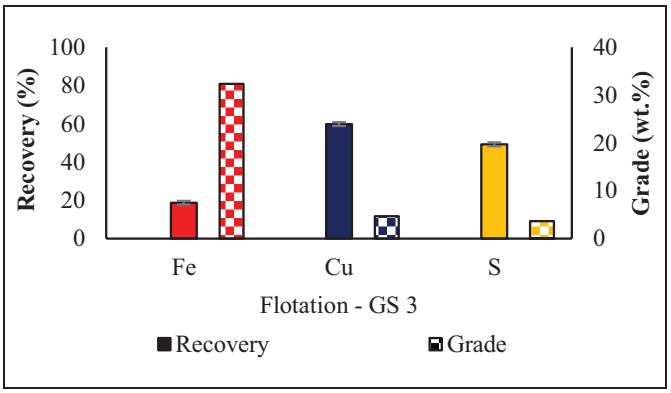

Figure 7. Flotation recovery and grade of the concentrate and middlings of gravity separation with a 1:5 S/L ratio

Table 7. Enrichment for Te, Au, and Ag for efficient collector and frother combinations

Baseline Flotation Conditions	Te	Au	Ag
EXP300422 (120g/t) + MIBC (50g/t)	2.25	1.57	1.42
EXP300422 (150g/t) + MIBC (50g/t)	2.00	1.41	1.27
EXP300422 (150 g/t) + terpineol (50g/t)	3.00	1.28	1.74
EXP300422 (150 g/t) + OREPREP X-237 (50g/t)	3.25	2.46	1.82
SPIX (30g/t) + MIBC (50g/t)	2.05	1.96	1.32
SPIX (90 g/t) + OREPREP X-237 (50g/t)	3.50	1.90	2.26
SPIX (150 g/t) + OREPREP X-237 (50g/t)	3.08	2.59	t
SPIX (90 g/t) + terpineol (50g/t)	2.88	1.49	1.85

previous research by Yano, 2012, Steadman et al., 2021, and Corchado & Alagha, 2023 suggested that Te, Au, Ag, Cu, and other valuables are 90% locked within larger pyrite grains as less than 20 µm in CT [26,33,34]. Therefore, this research investigated the froth flotation process for pyrite and other sulfides in CT using conventional reagents [31].

Subsequent baseline flotation experiments for pyrite concentration improved recovery rates and established a foundation for optimization research into other flotation parameters. The most efficient reagent combinations were identified, with 150 g/t SIPX and 50 g/t OREPREP X-237 yielding a 92.18% recovery for Te at a grade of 1.4 ppm, demonstrating substantial improvement. Tellurium, gold, and silver enrichments for the 150 g/t SIPX and 50 g/t OREPREP X-237 were 3.08, 2.59, and 1.98, respectively. Table 7 shows Te, Au, and Ag enrichment for the efficient collector and frother combinations from the pyrite baseline flotation experiments.

The introduction of a combination of gravity separation (GS) and froth flotation led to significant improvements in the pyrite concentration process. GS effectively removed gangue materials and enhanced the floatability of pyrite, suggesting that valuable elements locked within were enriched. Results indicated that the GS-C+M stream should be used as the flotation feed for the subsequent flotation experiments.

Table 8. Enrichment for Fe, Cu, and S for preconcentration and flotation experiments

Gravity Separation and Flotation Experiments	Fe	Cu	S
Flotation - GS 1 - C+M	1.55	3.01	2.19
Flotation - GS 2 - C+M	2.18	6.77	4.94
Flotation - GS 3 - C+M	1.98	5.80	3.14

In the flotation experiments, remarkable improvements were observed in Fe, Cu, and S recovery rates and grades, taken as an indicator of major sulfide concentration (pyrite and chalcopyrite). For instance, the GS 2-C+M had the highest enrichment of 2.18, 6.77, and 4.94 for Fe, Cu, and S, respectively. Therefore, these results suggested that GS 2-C+M would have a higher enrichment in pyrite, chalcopyrite, and associated Te-Au-Ag-bearing minerals. **Table 8** shows the Fe, Cu, and S enrichment for preconcentration and flotation experiments.

These results highlighted the success of the geometallurgical research approach in enhancing the recovery and the enrichment of Te, Au, and Ag from copper tailings, potentially transforming previously discarded material into a valuable resource.

CONCLUSIONS

The research into the enrichment feasibility of gold- and silver-tellurides from copper tailings has yielded promising results. The study addressed the growing demand for tellurium (Te), a critical element for solar energy technologies, by enhancing its recovery from existing supply chains by reprocessing copper tailings (CT). Baseline flotation experiments identified specific reagent combinations that achieved significant recoveries for Te, Au, and Ag, showing the potential to recover these valuable elements from copper tailings efficiently. Combining gravity separation (GS) and froth flotation experiments significantly improved the enrichment of Fe, Cu, and S (representative of pyrite and chalcopyrite in CT), transforming previously discarded materials into valuable resources. However, further optimization is suggested by the authors to increase valuables' overall recovery in the combined GS and froth flotation process.

These findings offer a promising outlook for addressing the increasing demand for critical minerals in sustainable energy production and various industries. Future research should optimize the process and scale it up for pilot-scale testing. This could be a turning point in the standard practices of efficiently recovering Te and other critical minerals. The feasibility of scaling up the process should be studied via a techno-economic analysis to understand the impact that recovering Au and Ag with Te has on the financial scaling-up costs for the process.

REFERENCES

[1] Gupta, V.; Biswas, T.; Ganesan, K. *Critical NonFuel Mineral Resources for India's Manufacturing Sector*; 2016;

[2] Nakano, J. *The Geopolitics of Critical Minerals Supply Chains*; Washington, D.C., USA, 2021;

[3] Kwarteng, K. Resilience for the Future: The UK's Critical Minerals Strategy Available online: www.gov.uk/government/publications/uk-critical-mineral-strategy/resilience-for-the-future-the-uks-critical-minerals-strategy (accessed on 9 October 2023).

[4] Bauer, D.J.; Nguyen, R.T.; Smith, B.J. *Critical Materials*; 2023;

[5] Wilkinson, J.; Champagne, F.-P. *The Canadian Critical Minerals Strategy*; Canada, 2022;

[6] O'sullivan, M.L.; Bordoff, J. *A Critical Minerals Policy for the United States*; 2023;

[7] Nassar, N.T.; Fortier, S.M. Methodology and Technical Input for the 2021 Review and Revision of the U . S . Critical Minerals List. *U.S. Geological Survey Open File Report* 2021, *2021–1045*.

[8] Meinert, L.D.; Robinson, G.R.; Nassar, N.T. Mineral Resources: Reserves, Peak Production and the Future. *Resources* 2016, *5*, 1–14, doi:10.3390/resources5010014.

[9] Nassar, N.T.; Kim, H.; Frenzel, M.; Moats, M.S.; Hayes, S.M. Global Tellurium Supply Potential from Electrolytic Copper Refining. *Resour Conserv Recycl* 2022, *184*, 106434, doi:10.1016/J.RESCONREC.2022.106434.

[10] Fortier, S.M.; Nassar, N.T.; Mauk, J.L.; Hammarstrom, J.M.; Day, W.C.; Seal, R.R. *Mining Engineering*. May 2020, pp. 30–45.

[11] Nassar, N.T.; Brainard, J.; Gulley, A.; Manley, R.; Matos, G.; Lederer, G.; Bird, L.R.; Pineault, D.; Alonso, E.; Gambogi, J.; et al. Evaluating the Mineral Commodity Supply Risk of the U.S. Manufacturing Sector. *Sci Adv* 2020, *6*, doi:10.1126/sciadv.aay8647.

[12] Nassar, N.T.; Barr, R.; Browning, M.; Diao, Z.; Friedlander, E.; Harper, E.M.; Henly, C.; Kavlak, G.; Kwatra, S.; Jun, C.; et al. Criticality of the Geological Copper Family. *Environ Sci Technol* 2012, *46*, doi:10.1021/es203535w.

[13] Fortier, S.M.; Nassar, N.T.; Kelley. Karen D.; Lederer, G.W.; Mauk, J.L.; Hammarstrom, J.M.; DayWarren C.; Seal, R.R. *SME*. 2021, pp. 32–47.

[14] DOE Critical Materials Strategy. 2010, 1–166.

[15] Federal Register *Executice Order 13953: Addressing the Threat to the Domestic Supply Chain From Reliance on Critical Minerals From Foreign Adversaries and Supporting the Domestic Mining and Processing Industries*; Federal Register, 2020; Vol. 85;.

[16] Nassar, N.T.; Alonso, E.; Brainard, J.L. *Investigation of U.S. Foreign Reliance on Critical Minerals—U.S. Geological Survey Technical Input Document in Response to Executive Order No. 13953 Signed September 30, 2020*; 2020;

[17] Parthemore, C. *Elements of Security: Mitigating the Risks of U.S. Dependence on Critical Minerals*; 2011;

[18] Moss, Ray.L.; Tzimas, E.; Willis, P.; Arenderof, J.; Thompson, P.; Chapman, A.; Morley, N.; Sims, E.; Bryson, R.; Pearson, J.; et al. *Critical Metals in the Path towards the Decarbonisation of the EU Energy Sector*; Office of the European Union: Lexembourg, 2013; ISBN 9789279303906.

[19] Peck, D. A Historical Perspective of Critical Materials, 1939 to 2006. In *Critical Materials: Underlying Causes and Sustainable Mitigation Strategies*; Erik Offerman,

S., Ed.; World Scientific Publishing Co.: Hackensack, NJ, 2019; Vol. 5, pp. 85–101.
[20] Kelley, K.D.; Huston, D.L.; Peter, J.M. *SGA News*. March 2021, pp. 1–5.
[21] Doulgeridou, A.; Amlund, H.; Sloth, J.J.; Hansen, M. Review of Potentially Toxic Rare Earth Elements, Thallium and Tellurium in Plant-Based Foods. *EFSA Journal* 2020, *18*, doi:10.2903/j.efsa.2020.e181101.
[22] Li, Z.; Qiu, F.; Tian, Q.; Yue, X.; Zhang, T. Production and Recovery of Tellurium from Metallurgical Intermediates and Electronic WasteA Comprehensive Review. *J Clean Prod* 2022, *366*, 132796, doi:10.1016/J.JCLEPRO.2022.132796.
[23] Moats, M.; Alagha, L.; Awuah-Offei, K. Towards Resilient and Sustainable Supply of Critical Elements from the Copper Supply Chain: A Review. *J Clean Prod* 2021, *307*.
[24] Goldfarb, R.J.; Berger, B.R.; George, M.W.; Seal II, R.R. *Tellurium*; US Geological Survey, 2017;
[25] Wang, S. Tellurium, Its Resourcefulness and Recovery. *JOM* 2011, *63*.
[26] Corchado-Albelo, J.; Alagha, L. Characterization of Tellurium, Gold, and Silver Minerals in Copper Porphyry Processing Streams. In Proceedings of the Minexchange SME 2023 Conference; Denver, CO, March 1 2023.
[27] Hrstka, T.; Gottlieb, P.; Skála, R.; Breiter, K.; Motl, D. Automated Mineralogy and Petrology – Applications of TESCAN Integrated Mineral Analyzer (TIMA). *Journal of Geosciences (Czech Republic)* 2018, *63*, doi:10.3190/jgeosci.250.
[28] Corchado-Albelo, J.L.; Alagha, L. Studies on the Enrichment Feasibility of Rare Earth-Bearing Minerals in Mine Tailings. *Minerals* 2023, *13*, 301.
[29] Actlabs Geochemistry Schedule of Services & Fees 2023 International. 2023, 9–11.
[30] Yan, D.S.; Hariyasa Selective Flotation of Pyrite and Gold Tellurides. *Miner Eng* 1997, *10*, doi:10.1016/s0892-6875(97)00012-5.
[31] Yang, W.; Wang, G.; Wang, Q.; Dong, P.; Cao, H.; Zhang, K. Comprehensive Recovery Technology for Te, Au, and Ag from a Telluride-Type Refractory Gold Mine. *Minerals* 2019, *9*, doi:10.3390/min9100597.
[32] Zhang, J.; Zhang, Y.; Richmond, W.; Wang, H.P. Processing Technologies for Gold-Telluride Ores. *International Journal of Minerals, Metallurgy and Materials* 2010, *17*, 1–10, doi:10.1007/s12613010-0101-6.
[33] Steadman, J.A.; Large, R.R.; Olin, P.H.; Danyushevsky, L. V.; Meffre, S.; Huston, D.; Fabris, A.; Lisitsin, V.; Wells, T. Pyrite Trace Element Behavior in Magmatic-Hydrothermal Environments: An LA-ICPMS Imaging Study. *Ore Geol Rev* 2021, *128*.
[34] Yano, R.I. Trace Element Distribution in Chalcopyrite-Bearing Porphyry and Skarn Deposits. *Master's Thesis, Reno, USA, University of Nevada* 2012.

24-036

Estimating Air Blast Velocity Using Optical Flow Algorithm

Vasu Gangrade
National Institute for Occupational Safety and Health, Pittsburgh, PA

ABSTRACT

Large-opening underground stone mines pose significant ground control challenges, including the risk of massive pillar collapses. These collapses can result in dangerous air blasts characterized by tremendous force and high velocity. Estimating the velocity of these air blasts proves challenging due to the absence of accurate air velocity instruments near the mine portals. To address this issue, this paper proposes a novel approach that leverages closed-circuit television camera footage from the mine. Specifically, it employs the optical flow algorithm implemented in Python to estimate the velocity of the air blasts, providing a valuable tool for assessing and mitigating risks in such mining environments.

INTRODUCTION

Underground limestone mines are generally mined using the room-and-pillar method. As the name suggests, the method involves forming a grid-like pattern of entries and crosscuts underground, and the stone deposit is divided into a series of pillars, which are left standing to support the roof of the mine. The method is specially challenging in stone mines as the entry sizes are very large ranging from 40–50 ft wide and 30–40 ft high entries. In addition to the entries, the underground stone mines also use benching. Benching involves further excavating the floor of the entries which increases the development height to 90–100 ft (Figure 1). Therefore, benching creates tall slender pillars in the underground stone mines which are high, but less wide (Figure 2). These pillars often form an hourglass shape and can collapse if the pillar cannot take the weight of the roof (Mark and Rumbaugh, 2022).

A pillar collapse happens when an array of pillars fails suddenly. Pillar collapses can occur with very little warning and can affect miners far away from the collapse (MSHA, 2023). Several factors can contribute to a pillar collapse, including excessive mining of adjacent rooms leading to increased stress on the pillars, geological faults or weaknesses in the surrounding rock, changes in the stress distribution within the mine due to excavation activities or subsurface factors, and inadequate pillar design or insufficient pillar size for the load they are supporting.

Figure 1. Typical large-opening stone mine with benching

Pillar collapse in underground stone mines presents a grave safety concern, as it endangers the lives of miners working not just in the affected area but everywhere near the mine. The sudden failure of support pillars can lead to catastrophic events, including roof collapses and falling debris, placing miners at immediate risk from the ground control event. The pillar collapse also leads to the formation of an air blast.